Astron. Astrophys. 348, 728–736 (1999)

ASTRONOMY AND ASTROPHYSICS

The chemical composition of the young, Inter-Cloud population

W.R.J. Rolleston[1], **P.L. Dufton**[1], **N.D. McErlean**[1,⋆], **and K.A. Venn**[2,⋆]

[1] Department of Pure and Applied Physics, The Queen's University of Belfast, Belfast BT7 1NN, N. Ireland, UK (R.Rolleston@qub.ac.uk)
[2] Macalester College, 1600 Grand Ave, St. Paul, MN 55105, USA (venn@clare.physics.macalester.edu)

Received 9 February 1999 / Accepted 4 June 1999

Abstract. High-resolution AAT spectroscopy and lower resolution spectrophotometry are presented for three early B-type stars that are members of the young, Inter-Cloud population between the Magellanic Clouds. These spectra have been analyzed using LTE model-atmosphere techniques, to derive the stellar atmospheric parameters and photospheric chemical compositions. The latter should reflect that of the *present-day* interstellar medium (ISM) within the Inter-Cloud Region (ICR).

From a differential analysis, the three ICR stars appear to have a mean metal abundance of ∼1.1 dex lower than their Population I Galactic analogues, and 0.5 dex lower than the SMC star (AV 304). Hence, the ICR gas *does* not reflect the present-day composition of either the SMC (or LMC) ISM. Age (and distance) estimates were obtained using the theoretical isochrones of Bertelli et al. (1994); these imply that the young, Inter-Cloud population has an age dispersion of at least 10–40 Myr, and provide evidence for a distance gradient across the ICR. We discuss our results within the context of recent numerical simulations of the gravitational interactions between the Galaxy–LMC–SMC, that predict that the ICR was tidally disrupted from the SMC some 200 Myr ago. If the SMC was chemically homogeneous, a comparison of the ICR abundance determinations with the SMC age-metallicity relationship would then imply that the formation of the ICR must have occurred ∼8.5 Gyr ago. Alternatively and more plausible, we postulate that the ICR gas formed from a mixture of SMC gas and an unenriched component. This is consistent with model-predictions that both a halo and disc component should have contributed to the material within the ICR during the tidal disruption.

Key words: stars: abundances – stars: atmospheres – stars: early-type – galaxies: Magellanic Clouds

1. Introduction

The Large (LMC) and Small (SMC) Magellanic Clouds are two small irregular galaxies orbiting our own Galaxy, with the LMC being approximately 3–10 times more massive than the SMC (Dopita 1990; Lequeux 1984). Canonical distance estimates for the LMC and SMC are ∼49 kpc and ∼60 kpc respectively (see Westerlund 1990), although recent studies by Udalski et al. (1998), using Hipparcos data, suggest that both galaxies are some 15% closer than previously assumed. The interactions between the LMC and SMC and that between the Clouds and the Galaxy are believed to have markedly influenced their evolutionary development (Gardiner & Noguchi 1996). Furthermore, the presence of a pair of such galaxies orbiting so close to our own Galaxy, will produce observable tidal features not seen in isolated pairs (Wayte 1991).

Extra-galactic H I gas was first detected in the direction of the Clouds by Kerr et al. (1954). It was later shown to extend well beyond the visible regions of each galaxy (Bok 1966) with a *bridge* of gas existing in the Inter-Cloud Region (Hindman et al. 1963). The enormous extent of the system was uncovered when the sequence of H I clouds forming the Magellanic Stream was detected (Mathewson et al. 1977, and references therein), extending as a long filament some 100° across the sky from the north-east corner of the SMC. Given the correlation between H I emission and stellar condensations, searches employing automatic scans of Schmidt plates have been undertaken for star formation in both the Magellanic Stream (Bruck & Hawkins 1983) and the Inter-Cloud Region (Irwin et al. 1985). Although the former have yielded largely negative results, Irwin et al. established the existence of a blue stellar link between the Clouds. Subsequent CCD photometry by Grondin et al. (1992, and references therein) and Demers & Battinelli (1998) have shown the Inter-Cloud associations (ICA) to contain massive, young (<16 Myr) stars at distances intermediate between those of the LMC and SMC.

For a number of years, we have been using young, B-type stars as tracers of the *present-day* metallicity in the Magellanic System. The spectral analyses of such objects yield reliable photospheric abundance estimates for the light elements such as C, N, O, Al, Mg & Si. These investigations have shown the interstellar medium within the SMC to be underabundant by approximately 0.7 dex (Dufton et al. 1990a; Rolleston et al. 1993) and the LMC by approximately 0.3 dex (Rolleston et al. 1996), which are consistent with abundance results from H II regions, A-type supergiants and most F–K supergiants as dis-

Send offprint requests to: W.R.J. Rolleston

⋆ Visiting Astronomer, Cerro Tololo Inter-American Observatory. CTIO is operated by AURA Inc., under contract to the National Science Foundation.

Table 1. Observational details of the programme stars.

Object	α (2000.0)	δ	V	$B-V$	E$(B-V)$[4]	SpT[5]	Association
DI 1162	02 27 38.90	−73 45 48.7	15.35[1]	−0.20[1]	0.08	B2	ICA 46 (IDK-2)
DI 1239	02 30 40.81	−74 04 45.3	15.24[2]	−0.31[2]	0.08	B1	ICA 55
DGIK 975	04 19 58.62	−73 52 26.2	15.05[3]	−0.19[3]	0.12	B2	ICA 76 (IDK-6)

References: (1) Grondin et al. (1990); (2) Demers & Irwin (1991); (3) Demers et al. (1991); (4) Demers & Battinelli (1998); (5) Rolleston (1999).

cussed recently in Venn (1998, 1999). Furthermore, Rolleston et al. (1993) presented tentative evidence for inhomogeneities in the chemical composition of the SMC, with an apparent greater metal deficiency being found for an object in its eastern wing. This is particularly interesting as the SMC wing protrudes into the ICR. More recently, Hambly et al. (1994) presented model-atmosphere analyses of two young B-type stars in the ICR and concluded that one star, DI 1194, exhibited a general metallicity deficiency of as much as 1.0 dex, similar to the composition of the SMC eastern wing star, IDK-D2.

These studies confirm that star-formation is ongoing in the ICR and is consistent with its material originating from the SMC. Unfortunately, only a small amount of observational data (viz. stellar distances/ radial velocities/ metallicities) exists for objects between the Magellanic Clouds. Hence, the star-formation mechanism, homogeneity and origin of the gas structures within the ICR are still unclear. Rolleston (1999) initiated an observational programme in order to address these issues. In December 1994, a low-resolution spectroscopic survey was performed using the SAAO 1.9-m for some 30 blue objects distributed across the ICR. From these spectra, seven objects were positively identified as having Magellanic-type radial velocities, early-B spectral types and hydrogen/ helium line-spectra that are consistent with that of luminosity class III–V objects. Subsequent high-resolution spectroscopy was obtained for three stars, for which we present the results of the model-atmosphere analyses in this paper. Details of the programme stars, including the spectral types deduced from the low-resolution study (Rolleston 1999) and references for the existing BV photometry, are given in Table 1.

2. Observations and data reductions

2.1. AAT high-resolution spectroscopy

The high-resolution spectroscopy presented in this paper was obtained with the 3.9-m Anglo-Australian Telescope (AAT) between 29$^{\rm th}$ November and 2$^{\rm nd}$ December 1995. The Royal Greenwich Observatory spectrograph (Stathakis & Johnston 1997), which is mounted at Cassegrain f/8, was operated with the 82 cm camera (blaze-to-collimator), the R1200B grating and a Tek 1K CCD. This instrumental configuration yielded a full-width-half-maximum resolution of approximately 0.6 Å. Two wavelength settings were required, viz. $\lambda\lambda$3910–4155 Å and $\lambda\lambda$4460–4705 Å, in order to observe the most important diagnostic lines for the determination of the stellar atmospheric parameters and photospheric abundances (see Sect. 3). Additionally, the blue spectral region facilitated the observation of interstellar absorption gas in Ca H&K. Stellar observations were sub-divided into 1200 s integrations, so as to minimize the effects of cosmic ray events, and these were bracketed by copper-argon arc exposures for wavelength calibration. Bias frames and flat-field exposures, the latter made using a quartz continuum lamp, were taken at the beginning and end of each night.

The two dimensional CCD images were reduced using standard procedures within IRAF (Tody 1986). Preliminary processing of the CCD frames such as overscan correction, trimming of the data section and flat-fielding were performed using the CCDRED package (Massey 1997), whilst cosmic-ray removal, extraction of the stellar spectra, sky subtraction and wavelength calibration were undertaken using tasks within the SPECRED package (Massey et al. 1992). After co-addition of the extracted spectra from the individual image frames, a signal-to-noise ratio of ∼60–70 was obtained in the stellar continua. Further manipulation of the stellar spectra, viz. radial velocity corrections, rectification of the stellar continuum and the measurement of equivalent widths for the metal and non-diffuse helium line-spectra, utilized the suite of routines provided by the spectral reduction package DIPSO (Howarth et al. 1994). Full details of these methods can be found in Rolleston et al. (1996) and references therein. The equivalent width data for the non-diffuse helium and metal lines can be obtained from the authors upon request.

2.2. CTIO spectrophotometry

A preliminary inspection of the metal-line spectra revealed that these features were intrinsically weak in all three programme stars (see Sect. 4.1). This precluded the observation of absorption lines from two ionization stages of the same element, which can be used to determine stellar effective temperatures. Additionally, Strömgren photometry which can also be used to estimate temperatures were unavailable for these objects.

Hence, spectrophotometry of the programme stars was obtained using the CTIO 1.5-m telescope and CSPEC spectrograph during the nights of 18$^{\rm th}$/19$^{\rm th}$ December 1997. The combination of Grating #26 and a Loral 1K CCD provided a full-width-half-maximum resolution of approximately 3.5 Å and a useful spectral coverage between approximately $\lambda\lambda$3530–5115 Å. The observations were performed using a wide 5″ slit in photometric conditions and these were bracketed with exposures of flux standards, viz. HR 9087, HR 718, HR 3454 and HR 1544. The initial CCD reductions to remove the 'detector characteristics'

Table 2. Stellar parameters.

Star	$T_{\rm eff}$ (K)	$\log g$ (dex)	ξ (km s^{-1})	Mass ($M_\odot$)	Age (Myr)	d (kpc)	Comparison	$T_{\rm eff}$ (K)	$\log g$ (dex)	ξ (km s^{-1})
DI 1162	20 500	3.6	5	9.7	38	44	HR 39	20 000	3.75	5
DI 1239	24 000	3.8	5	11.3	25	41	HR 1886	23 500	4.1	6
DGIK 975	20 000	3.6	5	9.3	41	35	HR 39	20 000	3.75	5
AV 304	26 500	3.9	10	12.9	10	42	HR 2387	26 000	3.8	10

and the extraction of wavelength calibrated spectra were processed using identical procedures to that described in Sect. 2.1. Flux calibration consists of two additional steps, an extinction correction and an instrumental sensitivity calibration, and these were applied within the DOSLIT task (Valdes 1992).

2.3. Comparison stars

High signal-to-noise échelle spectroscopy of bright, normal Population I B-type stars have been obtained previously with the 0.9-m coudé feed telescope at Kitt Peak National Observatory. These data provide a spectral coverage of $\lambda\lambda$3900–4700 Å at a full-width-half-maximum resolution of 0.1 Å. Stellar spectra were again extracted using similar techniques, and equivalent width estimates for the non-diffuse helium and metal-lines have been published by Hambly et al. (1997). The programme star, DI 1239, was also compared with our study of the SMC B-type dwarf, AV 304. Dufton et al. (1990a) presented the equivalent width data for these observations, that were obtained with the 3.9-m Anglo-Australian Telescope in November 1989 using the UCLES spectrograph, 79 lines mm^{-1} grating and the IPCS detector.

3. Data analysis

The methods used to derive the stellar atmospheric parameters are similar to those discussed by Rolleston et al. (1993, 1996). We have adopted theoretical results based on the ATLAS9 grid of line-blanketed model-atmospheres (Kurucz 1991) together with LTE radiative transfer codes. Although the assumption of a normal, Galactic Population I chemical composition is not appropriate for these Magellanic stars (see Sect. 4.1), our tests have shown that the use of such models should not lead to significant errors in the resultant model-atmosphere analyses (see Rolleston et al. 1993; Hambly et al. 1997).

3.1. Effective temperatures, surface gravities

Effective temperatures ($T_{\rm eff}$) were deduced for the programme stars by comparing model-atmosphere calculations with the observed flux calibrated spectra obtained at CTIO (see Fig. 1). The latter had first to be corrected for the effects of interstellar reddening; this was problematic as reliable optical (BV) photometry only exists for two of the stars, viz. DI 1162 (IDK-A7: Grondin et al. 1990) and DGIK-975 (Demers et al. 1991), and as the extinction in the Magellanic Clouds differs from the standard Galactic relation (Seaton 1979). Fortunately, the Inter-Cloud Associations (ICA) are located far enough from the main bodies of the SMC and LMC that they remain relatively unaffected by their internal reddenings (Grondin et al. 1990). Also, Demers & Battinelli (1998) have recently presented colour excesses for a number of ICAs of which our programme stars are either members or are situated within a few arcminutes on the sky, and we have adopted their values as given in Table 1. The slope of the stellar continuum is sensitive to the colour excess (over the observed wavelength range); typically, a change of 0.05 magnitudes in E($B-V$) corresponds to a change of approximately 1000 K in the derived stellar effective temperature. However, it is the Balmer discontinuity which is the most sensitive temperature diagnostic for these early-type stars and therefore, we placed greater weight on fitting the stellar continuum around this feature. The quality of our fits imply that the random errors in the estimation of the effective temperature should be $\leq$1000 K.

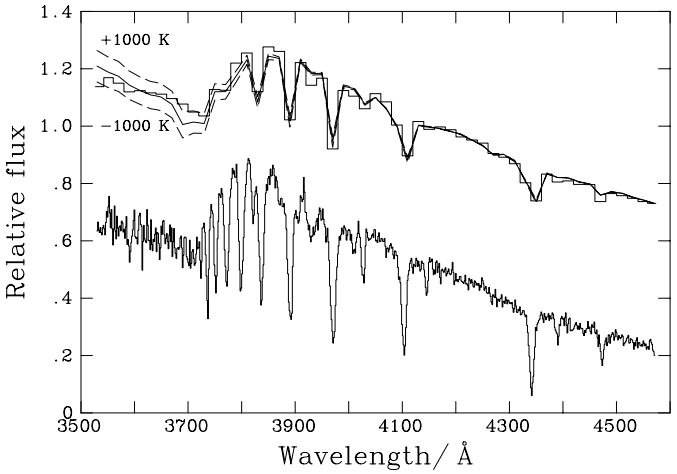

Fig. 1. (Bottom:) Part of the observed flux distribution for DI 1162, obtained using the CTIO 1.5-m telescope, and which has been dereddened as discussed in the text. Clearly visible are the lines of the Balmer series (from Hγ to H$_{12}$), the Balmer discontinuity and the neutral helium-line spectrum. (Top:) The dereddened flux distribution for DI 1162 is shown (histograms) rebinned to the resolution of the LTE model flux distributions. Theoretical spectra are superimposed for the adopted atmospheric parameters of DI 1162 (solid curve), viz. $T_{\rm eff} = 20\,500$ K, $\log g = 3.6$, and for $\triangle T_{\rm eff}$=$\pm$1000 K. This figure illustrates the ability of our methods to determine stellar effective temperatures to an accuracy of $\pm$1000 K.

Table 3. Absolute abundances of the programme stars.

Star	He	C	N	O	Mg	Al	Si
DI 1162	10.81±0.05	7.06±0.33	6.70	8.00±0.13	6.13	...	6.81±0.06
DI 1239	10.92±0.14	7.21	< 7.19	7.76±0.28	6.32	< 5.86	6.04±0.04
DGIK 975	10.83±0.05	<6.68±0.25	6.74	8.04±0.21	6.05	< 5.76	6.22±0.15
AV 304	10.9±0.1	6.85	6.89±0.17	8.10±0.16	6.84	< 5.53	6.73±0.02
Normal B-stars	11.00	8.20	7.81	8.68	7.38	6.45	7.58

Note: Errors (where quoted) refer to the standard deviation of abundance estimates obtained from individual lines. Uncertainties on the single measurements should be typically less than 0.2 dex (see Sect. 3.1).

Table 4. Differential abundance analysis.

Star	He	C	N	O	Mg	Al	Si	**Mean**
DI 1162	+0.05	−0.96±0.30	−1.14	−1.01±0.11	−0.98	...	−0.96±0.11	**−1.01±0.08**
DI 1239	...	−0.60	< -0.42	−1.12±0.27	−0.78	< -0.27	−1.28	**−1.06±0.26**
DGIK 975	$+0.00 <$	−1.34±0.23	−1.10	−0.98±0.26	−1.06	< -0.37	−1.46±0.21	**−1.19±0.20**
		−0.97±0.37	**−1.12±0.03**	**−1.04±0.07**	**−0.94±0.14**	**...**	**−1.23±0.25**	**−1.06±0.12**
AV 304	...	−0.58	< -0.91	−0.46±0.11	−0.46	...	−0.57±0.06	−0.60±0.18

Surface gravities were primarily deduced by fitting the theoretical profiles to the normalized AAT spectra of the Hϵ and Hδ lines; where the theoretical calculations have adopted the line-broadening theory of Vidal et al. (1973). It was also possible to determine surface gravity estimates from the low-resolution CTIO spectra using the Hϵ, Hδ, Hγ and Hβ line profiles. For all three programme stars, these estimates were consistent with those obtained from the high-resolution AAT spectra. The determination of these two atmospheric parameters is iterative, as the value deduced for the effective temperature depends to some extent on the adopted value of the surface gravity and vice-versa. However, the number of iterations was small as the Balmer discontinuity and the Balmer profiles are good indicators of effective temperature and surface gravity respectively.

The adopted atmospheric parameters are listed in Table 2 together with those for the corresponding bright, Galactic comparison stars. Effective temperature estimates were obtained for the latter from the Strömgren reddening free $[u-b]$ index using the calibration of Napiwotzki et al. (1993) with further details being given in Hambly et al. (1997). In order to test the validity of our inter-comparisons, we obtained spectrophotometry for 4 early B-type stars for which Strömgren temperatures have been determined previously, viz. HR 1887 (B0.5V), HR 1781 (B1.5V), HR 1923 (B2IV-V) and HR 1765 (B2IV-V). Effective temperatures were deduced from the flux calibrated spectra using the procedures described above and for the adopted colour excesses, E$(b-y)$, of Cunha & Lambert (1992), whilst surface gravities were inferred from the Hϵ, Hδ, Hγ and Hβ line profiles. Our spectrophotometric temperatures differed from the Strömgren temperatures of Cunha & Lambert (1992) by less than 500 K, while the difference in the two sets of surface gravity estimates ($\log g$) were approximately 0.05 dex. Hence, we conclude that the adoption of photometric temperatures for our Galactic comparison stars will not lead to significant systematic errors in the differential abundance analyses (see Sect. 4.1).

Rolleston et al. (1993) previously analysed the SMC star AV 304, and their effective temperature (determined from the Si III/ Si IV ionization balance) and surface gravity estimates have been adopted here, see Table 2. They also presented a differential study of AV 304 relative to the Galactic B0.5 V star HR 6165 (τ Sco). However, this object has an effective temperature of 30 500 K which is some 4000 K hotter than that of AV 304. In order to minimize the introduction of systematic errors into the differential abundance analysis, we have reanalysed AV 304 relative to the Galactic star HR 2387 which exhibits very similar atmospheric parameters (see Table 2).

3.2. Microturbulence

In early B-type stars, microturbulent velocities ($v_{\rm t}$) can be determined from, for example, their O II line-spectra by removing the dependence of the derived oxygen abundance upon the observed line-strengths (see Lennon et al. 1988). Unfortunately, the intrinsic weakness of the metal-line spectra for the programme stars (see Sect. 4.1) precluded any such measurement. However, the O II line-spectra in the Galactic comparison stars were of such a high quality that it was possible to determine reliable equivalent-width estimates for line-strengths of 10mÅ. The derived microturbulent velocities are tabulated in Table 2 for HR 39 and HR 1886, which are consistent with the canonical value of $5\,{\rm km\,s^{-1}}$ that has been found previously from similar LTE analyses of B-type main-sequence stars (Hardorp & Scholz 1970; Dufton et al. 1990b). Therefore, we have adopted our estimate for the microturbulent velocity of the corresponding standard star in the analysis of the programme objects. This seems reasonable, given that we have carefully selected Galactic comparison stars that display very similar atmospheric param-

eters to that of the ICR stars. In any case, the intrinsic weakness of the metal-line spectra for the latter significantly reduces the effect of errors in the adopted value of the microturbulence on the resultant abundance determinations (see Sect. 4.1).

A microturbulent velocity of 10 km s^{-1} was determined for AV 304 from a re-analysis of the oxygen line-spectrum. This was based on the observation of approximately 30 O II absorption features. This is also compatible with the value derived for the Galactic comparison star HR 2387 (see Table 2).

3.3. Stellar $v \sin i$

Stellar projected rotational velocities ($v \sin i$) were estimated by convolving theoretically generated spectra with rotational broadening functions until they matched the observations. It should be noted that this procedure accounts for the effect of instrumental broadening. However, $v \sin i$ estimates deduced from the hydrogen/ helium line-spectra were systematically larger than those inferred from the metal-line spectra for all three programme stars. This was particularly the case for DGIK 975 where it was impossible to simultaneously fit the weak metal and stronger hydrogen lines with the same broadening parameters. Additionally for this star, the metal lines gave a significantly larger value for $v_{\rm lsr}$ (210 km s^{-1}) than that obtained from the hydrogen and helium line profiles (180 km s^{-1}). A closer examination revealed that a positive correlation existed between the formation depth of the line core and the derived radial velocity of the absorption feature. This may be evidence for a stellar wind; but given the near main-sequence status of DGIK 975 and its B2 spectral type – a wind of such magnitude is rather unlikely. However the estimate from the weak metal lines, the cores of which have formed at larger optical depths, will probably better represent the radial velocity of DGIK 975 and is the value quoted in Table 6. This line shift may at least partially explain the difference in implied rotational broadening required for DGIK 975. However, no such line shifts are found in the other two stars and the (admittedly smaller) discrepancies are rather puzzling. Hence we have re-examined our data reduction/ spectral analysis procedures for possible sources of error. After exhaustive tests, we do not believe that the afore-mentioned discrepancy is the result of an incorrect treatment of the observational data. Additionally, we find no evidence of binarity or composite spectra in either our high-resolution AAT spectroscopy or lower resolution spectrophotometry. On the contrary, the atmospheric parameters and chemical compositions obtained from these data are internally consistent for each star, while the results for all three stars are compatible within our error estimates (see Sect. 4.1). Hence, although the different rotational broadening required for the hydrogen/ helium and metal-line spectra remains unresolved, we do not expect it to seriously compromise the model-atmosphere analyses.

3.4. Magellanic System membership

It is important to confirm that the programme stars are associated with the gas enveloping the Magellanic Clouds. Primarily, two criteria were used to confirm their membership, viz. stellar radial velocities and interstellar absorption lines. Radial velocities deduced from the high-resolution AAT spectra (see Table 6) were corrected to the local standard of rest ($v_{\rm lsr}$) and are consistent with the estimates of 136 km s^{-1} and 261 km s^{-1} for the LSR velocities of the SMC (Hardy et al. 1989) and LMC (Luks & Rohlfs 1992) respectively. The interstellar Ca II H&K features were observed in the stellar spectra. For all the programme stars, it was possible to identify absorption components due to both Galactic low-velocity gas clouds and material associated with the Magellanic System (see, for example, Wayte 1990). Hence, it would appear that our targets are indeed members of the Clouds.

Stellar masses, evolutionary ages and distances (see Table 2) have also been deduced from the adopted atmospheric parameters using methods as discussed in, for example, Rolleston et al. (1997). We have selected the theoretical isochrones published by Bertelli et al. (1994) for Z=0.004 and Z=0.001, which brackets the metallicities found for the Inter-Cloud stars (see Sect. 4.1). Thus, our distance estimates are expected to be slightly less than those derived by, for example, Demers & Battinelli (1998), because they adopted isochrones of higher metallicity (Z=0.004) which results in the main-sequence being brighter and thus further away. Unfortunately, our absolute distance estimates may also be subject to systematic errors – and may underestimate the true values by upto 30% (see Rolleston et al. 1996). This is the consequence of an inadequate treatment of the Balmer lines' wings in LTE which leads to an overestimate of the stellar surface gravity. Hence, we have not included the stellar distance as a primary membership criterion, although these are clearly compatible with the programme stars being associated with the Magellanic System (see Table 6).

3.5. Photospheric abundances

The adopted atmospheric parameters (listed in Table 2) were used to derive absolute LTE abundances for both the programme

Table 5. Differential analysis of DI 1239 relative to AV 304.

Species	$\triangle$[X/H]
O II	-0.50 ± 0.30
Mg II	-0.52
Si III	-0.69

Table 6. Properties of the Inter-Cloud gas.

Object	Age (Myr)	d (kpc)	$v^{*}_{\rm lsr}$ (km s^{-1})	$v^{\rm CaK}_{\rm lsr}$ (km s^{-1})	$W_{\rm CaK}$ (mÅ)
IDK-D2	28	65	+170	+156	159
DI 1162	38	44	+165	+186	190
DI 1194	28	67	+148	+169	168
DI 1239	25	41	+152	+176	269
DI 1388	9	37	+137	+197	42
DGIK 975	41	35	+210	+172	133

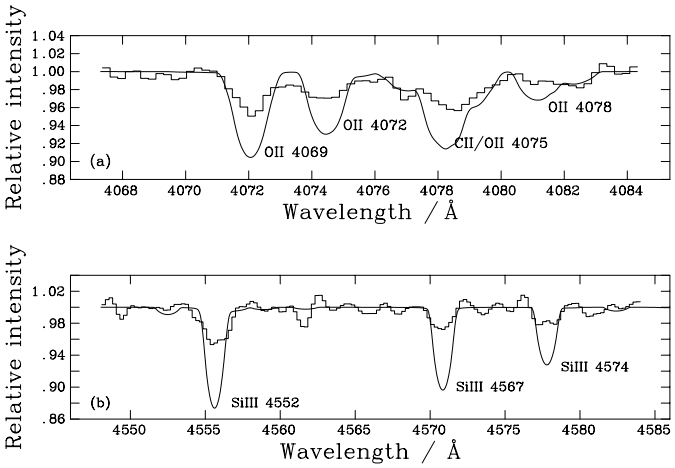

Fig. 2. Examples of the metal-line spectra (histograms) observed for DI 1162, for spectral regions including **a)** O II lines and **b)** Si III lines. Theoretical profiles (smooth curves) have been generated using the adopted atmospheric parameters derived for DI 1162 and the metal abundances found in the Galactic comparison HR 39. Comparison between the theoretical and observed line-strengths clearly illustrate the large metal deficiencies found for the ICR stars.

and comparison stars using procedures similar to those described in Dufton et al. (1990a) and Rolleston et al. (1997). Detailed line-by-line differential abundances were also performed relative to the 'normal' composition Galactic analogues HR 39 and HR 1886. Additionally, we have re-analysed the metal-line spectrum of the SMC star AV 304 (which should exhibit a metallicity typical of the present-day SMC) relative to HR 2387. The validity for using these bright Galactic disk B-type stars as standards of Population I chemical composition has been verified by Hambly et al. (1997).

4. Discussion of results

4.1. The chemical composition of the ICR stars

The model-atmosphere analyses are summarized in Tables 3, 4 and 5, the first presenting absolute abundances on a logarithmic scale with [H]≡12.0 dex, the other two listing differential abundances again on a logarithmic scale; errors (where quoted) refer to the sample standard deviations. A typical observational uncertainty of ±20mÅ in the equivalent-width estimate of an individual line would lead to an abundance error of ±0.3 dex. Additionally, the effect of changing the atmospheric parameters by their error estimates was considered, viz. $\triangle T_{\rm eff} \sim \pm 1000$ K, $\triangle \log g \sim \pm 0.2$ dex and $\triangle \xi \sim \pm 3\,{\rm km\,s^{-1}}$, and led to changes in the absolute abundance estimates by less than 0.2 dex. For the differential analyses, the atmospheric parameters of the relevant comparison star were derived using a similar technique as for the programme targets (see Sect. 3.1). This should reduce the effect of systematic errors in the estimates of the atmospheric parameters, while uncertainties in the adopted atomic data will also be less important. Additionally, simplifications in the model-atmosphere analyses (eg. the assumption of LTE) should also be less significant for the differential abundances.

The absolute abundances for the three Inter-Cloud stars and AV 304 are given in Table 3. For comparison purposes, we have listed the mean values reported by Gies & Lambert (1992) for a sample of 39 early B-type stars found in the local field, namely non-LTE abundances for He, C, N, O, Al and Si. The non-LTE abundance for Mg has been taken from Kilian (1994) for 21 unevolved B-type stars in the local field and the Ori OB1, Sco-Cen and Sgr OB1 associations. However, the atmospheric parameters of our programme stars are somewhat cooler than those used in these studies and different equivalent-width datasets have been used to derive the individual element abundances. Hence, for these reasons and those discussed above, it is more instructive to compare the differential abundances presented in Table 4.

All three ICR stars appear to have absolute helium abundances that are similar to that found for Galactic B-type stars. Indeed, the differential abundances imply that there are no significant differences between the helium content of the programme stars and their Galactic analogues. Unfortunately, the weakness of the metal-line spectra only permitted the observation of relatively few absorption features, viz. 2 C II, 1 N II, ∼8 O II, 1 Mg II and 3 Si III lines; however, the results are encouragingly self-consistent (see Table 4). For each ICR star in turn, individual element differential abundances lead to a mean metallicity that has a standard deviation of 0.2 dex. Thus, we are confident that the mean differential metallicity given in the last column of Table 4, can be taken as being representative of the composition of the local environment within the ICR. Furthermore, our results do not show significant variations between the mean photospheric compositions derived for the three stars, despite their quite different positions across the ICR (see Fig. 3). There is some marginal evidence to suggest that the carbon abundance may vary, cf. DI 1239 and DGIK 975. However, the higher estimate found for DI 1239 was based on the C II 3920 Å line alone, and the observational uncertainty in this case may be as large as 0.4 dex.

The most striking result is the magnitude of the metal deficiency observed in the ICR stars, viz. -1.06 ± 0.12 dex relative to normal, Galactic comparison stars. Our previous analyses of similar young, B-type stars in the Magellanic Clouds yield mean deficiencies of -0.7 dex and -0.25 dex for the SMC and LMC respectively. Thus the ICR objects would appear to have a metal content that is significantly lower than even the SMC. For this reason, we re-analzed our best target in the SMC (AV 304) relative to a new Galactic comparison star (HR 2387) with very similar atmospheric parameters (see Table 2) – yielding a new metal underabundance of 0.60±0.18 dex. These results suggest that the ICR objects are some 0.5 dex more deficient in the light elements than their analogues in the SMC. As DI 1239 and AV 304 possess approximately similar atmospheric parameters, we also performed a line-by-line differential analysis of DI 1239 relative to the latter. Unfortunately, the equivalent-width datasets for these two objects have only 3 O II, 1 Mg II and 1 Si III line in common. The results of this direct comparison (see Table 5) also yield a greater underabundance of 0.6±0.1 dex for DI 1239. Hence, we conclude that the present–day composition of gas in

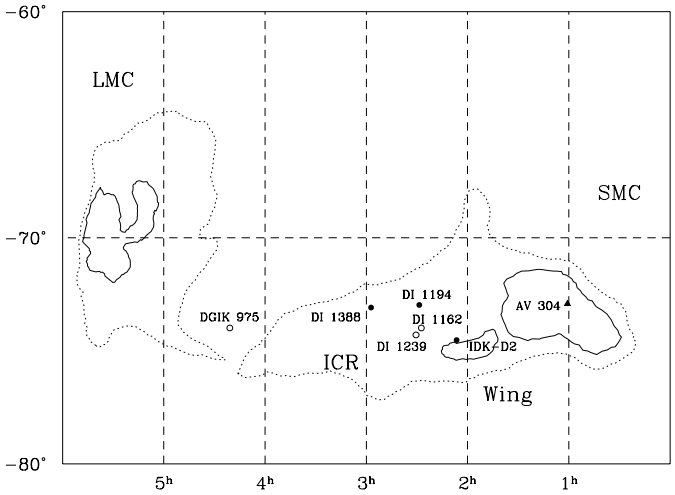

Fig. 3. A schematic diagram of the LMC, SMC and the Inter-Cloud Region (ICR). Solid lines define the stellar concentrations within the Magellanic Clouds, while the dashed lines show the H I envelopes of the Magellanic System. The positions of the three programme stars are designated by open circles. Also shown are the positions of three ICR objects (solid circles) previously studied by Rolleston et al. (1993) and Hambly et al. (1994), and the SMC comparison star AV 304 (solid triangle; Rolleston et al. (1993).

the Inter-Cloud Region is approximately 0.5 dex more deficient than the gas in the principle sites of star-formation in the SMC.

4.2. Interstellar observations of the ICR gas

Previously, we have obtained AAT UCLES spectra for three B-type stars in the ICR, viz. IDK-D2 (Rolleston et al. 1993) and DI 1194, DI 1388 (Hambly et al. 1994). Although these observations and the new stellar spectra presented here were principally used to measure stellar features, they also provide the first detection of interstellar absorption lines from the ICR gas. In Table 6, we present the radial velocity and equivalent-width of the Ca II K interstellar absorption for the Magellanic gas component towards the six ICR sight-lines. The former can be compared with the stellar radial velocity, where all have been corrected to the Local Standard of Rest ($v_{\rm lsr}$). For the two coolest stars (IDK-D2 and DI 1194) that have effective temperatures of approximately 14 000 K, there might be a significant stellar contribution to the Ca II K equivalent-width measurement. We estimate that this contribution may be as large as 50 mÅ – assuming that the stellar photospheres of these objects are deficient in calcium by -1.1 dex relative to that found in our Galactic comparison stars. There is also some observational evidence for such a contamination, as the spectra show broader Ca K components (at Magellanic-type velocities) than the Galactic absorption towards these two sight-lines. However, the low signal-to-noise obtained in the stellar continuum of these UCLES IPCS observations, do not allow us to distinguish between multiple Magellanic interstellar components and a significant stellar contribution. The sight-line towards DI 1388 shows a significantly weaker absorption than the other sight-lines. This may be evidence for a lower gas density in this region. However, a conclusive explanation must await the analysis of UV HST and radio ATCA observations (see Lehner et al. 1999). Neglecting the IDK-D2 and DI 1194 sight-lines, as these radial velocity estimates of the ICR gas may be affected by a possible stellar component, there does not appear to be a correlation between the observed LSR velocity and position across the ICR.

The Ca II K velocities are also in good agreement with H I velocities available near to our programme stars (see Lehner et al. 1999). Moreover, the stellar radial velocities are also comparable to those of the interstellar gas (see Table 6). For DGIK 975, the observed stellar radial velocity of 210 km s^{-1} is approaching 'LMC–type' velocities. This is interesting as Demers & Battinelli (1998) report a radial velocity estimate of $\sim$270 km s^{-1} for another object in ICA 76, viz. A6-986. However, there does appear to be a paradox here. If ICA 76 formed from material which originated in the LMC – then it might be expected to find this reflected in the derived abundance pattern for DGIK 975. Additionally, the LSR velocity of the ICR gas towards DGIK 975 is 'SMC–like', and there is no evidence of a LMC component.

4.3. Evolutionary history of the Inter-Cloud Region

Stellar evolutionary ages were derived for our six target stars as discussed in Sect. 3.4, and these clearly show that star-formation has occurred very recently across the entire ICR (see Table 6). Our results suggest that the ICAs have an age dispersion of at least 10–40 Myr, which is in reasonable agreement with the photometric study of Demers & Battinelli (1998). They concluded that star-formation started in the SMC wing and continued for $\sim$40 Myr before propagating across the ICR. Unfortunately, our stellar distances for the near main-sequence objects may be systematically underestimated, due to the assumption of LTE (see Sect. 3.4). Moreover, the distance estimates obtained for the two luminosity class II objects (IDK-D2 and DI 1194) will also be affected by non-LTE effects plus theoretical uncertainties in the stellar evolutionary calculations (see Bertelli et al. 1994). Hence, it is probably not worthwhile attempting to use our *absolute* distance estimates to constrain the distance of the ICR material. However, *relative* distances should be reliable for stars with similar atmospheric parameters. Then neglecting the two mid-B luminosity class II objects, we see that a distance gradient (see Table 6) is observed across the ICR with DGIK 975 (in ICA 76) being some 20% closer than DI 1162 (in ICA 46). This is compatible with the concept of a 'bridge' of material connecting the eastern wing of the SMC to the outer western halo of the LMC, and again is in agreement with the findings of Demers & Battinelli (1998).

It is interesting to note that Rolleston et al. (1993) presented 'tentative' evidence for chemical inhomogeneities in the SMC, and in particular, a greater underabundance of metals in the SMC wing. Carbon (-1.2 dex) and magnesium (-1.1 dex) deficiencies in the wing star IDK-D2 are remarkably similar to that observed for the 3 ICR stars, and are consistent with the hypothesis that both the SMC wing and ICR possess a common

origin. However, if the Inter-Cloud gas was tidally disrupted in recent history from the main body of the SMC, then it is to be expected that this material would reflect the present–day SMC abundance pattern. Our results clearly show that the material within the ICR does not reflect the present-day metallicity of either the SMC or LMC. Furthermore, our study does not show any evidence of an SMC–LMC abundance gradient across the ICR. The material would appear to be chemically homogeneous within our errors, and if anything, DGIK-975 (which is closer to the LMC) may be marginally more deficient in carbon and silicon.

The gravitational interactions between the Galaxy–LMC–SMC are thought to have produced several tidal features such as the Magellanic Stream and the ICR, and distorted the internal structures of the Clouds. Several groups have modelled some or all of these interactions. For example, Kunkel et al. (1994) neglected the gravitational influence of the Galaxy and adopted an unbound orbit for the SMC with respect to the LMC. The numerical simulations of Murai & Fujimoto (1980) and Gardiner & Noguchi (1996) are based on models in which the Galaxy has an extended massive halo, and the Magellanic Clouds have polar orbits with the Clouds leading the Magellanic Stream. Although the individual simulations lead to different interpretations of the kinematics of the Magellanic system, they all generally reproduce the main features of the internal structures of the Clouds and a tidal bridge and tail structure in the ICR. These latter tidal structures are believed to have been generated by the recent near-collision of the LMC/SMC about 200 Myr ago. In an interaction of this type (Toomre & Toomre 1972), the more massive LMC is regarded as the "perturber" and the SMC is the "victim". Leading the lower mass SMC and falling inward towards the LMC, a bridge begins to detach just prior to pericentric passage; while lagging behind the SMC, a tail begins to form at about the same time (Kunkel et al. 1994). These gas structures constitute the ICR and are seen overlapped in the sky, with the tail material being more distant than the bridge (Gardiner & Noguchi 1996).

We can use our abundance estimates of the ICR gas to place constraints on these models. First, we shall assume that the material, from which the ICR stars formed, originated in the SMC disc. For dwarf galaxies like the SMC, the disc material should be chemically homogeneous provided the star–formation rate is relatively constant and the infall of external material insignificant. This is due to the expanding gas shells from evolving massive stars that thoroughly mix the ISM over galaxy-wide scales on time-scales considerably less than the Hubble time (Kobulnicky & Skillman 1997). The chemical enrichment of the Magellanic Clouds has been investigated using integrated properties of star clusters (see Bica et al. 1986). More recently, Da Costa & Hatzidimitriou (1998) determined an SMC age-metallicity relationship using Ca II triplet spectra of individual red giants, in seven star clusters with ages between ∼4–12 Gyr. They concluded that the enrichment of the SMC could be explained by a simple 'closed system' model of chemical evolution, scaled to the present-day mean metallicity (−0.6 dex), gas mass fraction (0.36) and formation epoch (∼15 Gyr). The enrichment history consists of a rapid ($\tau \sim 3$ Gyr) initial metallicity increase, followed by a more modest rise starting ∼10 Gyr ago and continuing until the present epoch. Given the scenario whereby the SMC is a thoroughly mixed system, then comparison of our abundance determinations for the ICR with the age-metallicity relationship of Da Costa & Hatzidimitriou (1998), imply that the tidal structures within the ICR were disrupted approximately 8.5 Gyr ago. However, investigations of the initial mass function (IMF) within the ICR do not show any evidence of star–formation at such an early epoch (Demers & Battinelli 1998). Furthermore, if the formation of the ICR occurred ∼8.5 Gyr ago, then the recent simulations of the Magellanic Cloud orbits (Gardiner & Noguchi 1996) imply that the ICR has survived several pericentric passages of the SMC to the LMC.

Alternatively, the SMC is not a well mixed system. There is some evidence for this. For example, Da Costa & Hatzidimitriou (1998) present observational evidence for two intermediate age open clusters that have metallicities ∼0.5 dex lower than that expected from the mean age-metallicity relationship. These objects (Lindsay 113 and NGC 339) are situated in the south and extreme east of the SMC respectively. Furthermore, there has been considerable controversy regarding the chemical composition of the young, populous cluster NGC 330 (see Lennon et al. 1996), which may be up to 0.3 dex more metal-poor than field objects of comparable age (although recent differential analyses of cluster and field F–K type supergiants do not show significant differences in the cluster abundances, Hill 1998). Bertelli et al. (1992) and Gallagher et al. (1996) present some evidence for the outer halo of the LMC to be more metal-poor (−0.7 dex) than the adopted LMC metallicity of −0.3 dex. Hence, we may postulate that the ICAs formed from a mixture of SMC gas with a metal content appropriate to that of the ISM at ∼200 Myr ago, and diluted by a component with a lower abundance. This would be consistent with the scenario whereby the close encounter of the LMC tidally disrupted gas particles from both the SMC disc and halo. Given that the ICAs formed from gas approximately 0.5 dex more deficient in metals than the SMC, the required dilution factors range from 0.68 for unenriched (primordial) gas to 1.00 for gas with a metal content equal to that of the ICR. It is interesting to compare this scenario with the model predictions of Gardiner & Noguchi (1996). They predict that the ratio of particles in the tidal bridge to the number of particles in the tail originating from the disc and halo will be 1.4 and 3.3 respectively. Also, while the halo component makes a definite contribution to the bridge but only a very weak contribution to the tail, the disc component makes a significant contribution to both the bridge and tail. Hence this model would imply that our targets are likely to be situated in the bridge and that higher metallicity objects would be present in the tail.

Although, Gardiner & Noguchi (1996) do not provide ratios for the number of halo to disc particles in the tidal bridge and tail, their simulations illustrate that this hypothesis is plausible. However, further radial velocity and metallicity determinations for young, early-type stars in these tidal structures are necessary, in order to constrain both the complex dynamical and chemical evolutionary history of the ICR.

5. Conclusions

1. The three Inter-Cloud Region (ICR) stars display photospheric abundances that are deficient by -1.06 ± 0.12 dex relative to normal, Population I Galactic comparison stars. Furthermore, a differential analysis with respect to the SMC star AV 304, show the ICR stars to be more metal-poor by $\sim$0.5 dex.
2. The determination of stellar ages using the evolutionary calculations of Bertelli et al. (1994) imply that the Inter-Cloud Associations (ICA) have an age dispersion of at least 10–40 Myr. Moreover, our distance estimates support the view that a distance gradient is present across the ICR, with the LMC-side being some 20% closer than the SMC wing.
3. Based on the results of the model-atmosphere analyses, we conclude that the ICR material does not reflect the present-day composition of the principle sites of star-formation within either the LMC/SMC.
4. A comparison of our abundance determinations for the ICR with the SMC age-metallicity relationship of Da Costa & Hatzidimitriou (1998) was used to estimate the epoch of formation for the ICR. Assuming that the SMC is a well mixed system, then we infer that the ICR gas was tidally disrupted from the SMC $\sim$8.5 Gyr ago, although this would appear to be inconsistent with theoretical models and the initial mass function of the ICR.
5. Alternatively, we postulate that the ICR gas formed from a mixture of SMC gas and an unenriched component. For material which is approximately a factor of 3 more deficient in metals than the SMC, the required dilution factor ranges from 0.68 for unenriched (primordial) gas to unity for gas with a metal content equal to that of the ICR.

Acknowledgements. We would like to thank the staffs of the Anglo-Australian Observatory and Cerro Tololo Inter-American Observatory for their assistance in obtaining the observational data. Data reduction and analysis was performed on the PPARC funded N. Ireland STARLINK node. WRJR acknowledges financial assistance from the PPARC and NDME was funded by the Department of Education for Northern Ireland. KAV is supported by a Clare Boothe Luce professorship and is grateful to Macalester College for travel support to CTIO.

References

Bertelli G., Mateo M., Chiosi C., Bressan A., 1992, ApJ 388, 400
Bertelli G., Bressan A., Chiosi C., Fagotto F., Nasi E., 1994, A&A 106, 275
Bica E., Dottori H., Pastoriza M., 1986, A&A 156, 261
Bok B.J., 1966, ARA&A 4, 95
Bruck M.T., Hawkins M.R.S., 1983, A&A 124, 216
Cunha K., Lambert D.L., 1992, ApJ 399, 586
Da Costa G.S., Hatzidimitriou D., 1998, AJ 115, 1934
Demers S., Battinelli P., 1998, ApJ 115, 154
Demers S., Irwin M.J., 1991, A&AS 91, 171
Demers S., Grondin L., Irwin M.J., Kunkel W.E., 1991, AJ 101, 911
Dopita M.A., 1990, In: The Interstellar Medium in Galaxies. Proc. of the 2$^{\rm nd}$ Teton Conference, Kluwer, Dordrecht, p. 437
Dufton P.L., Fitzsimmons A., Howarth I.D., 1990a, ApJ 362, L59
Dufton P.L., Brown P.J.F., Fitzsimmons A., Lennon D.J., 1990b, A&A 232, 431
Gallagher J.S., Mould J.R., de Feijter E., et al., 1996, ApJ 466, 732
Gardiner L.T., Noguchi M., 1996, MNRAS 278, 191
Gies D.R., Lambert D.L., 1992, ApJ 387, 673
Grondin L., Demers S., Kunkel W.E., Irwin M.J., 1990, AJ 100, 663
Grondin L., Demers S., Kunkel W.E., 1992, AJ 103, 1234
Hambly N.C., Dufton P.L., Keenan F.P., et al., 1994, A&A 285, 716
Hambly N.C., Rolleston W.R.J., Keenan F.P., Dufton P.L., Saffer R.A., 1997, ApJS 111, 419
Hardorp J., Scholz M., 1970, ApJ 154, 1111
Hardy E., Suntzeff N.B, Azzopardi M., 1989, ApJ 344, 210
Hill V., 1998, In: Chu Y.H., Suntzeff N. (eds.) New Views on the Magellanic Clouds. ASP Conf. Series, San Francisco
Hindman J.V., Kerr F.J., McGee R.X., 1963, Aust. J. Phys. 16, 570
Howarth I.D., Murray J., Mills D., 1994, Starlink User Note, No. 50.15
Irwin M.J., Kunkel W.E., Demers S., 1985, Nat 318, 160
Kerr F.J., Hindman J.V., Robinson B.J., 1954, Aust. J. Phys. 7, 297
Kilian J., 1994, A&A 282, 867
Kobulnicky H.A., Skillman E.D., 1997, ApJ 489, 636
Kunkel W.E., Demers S., Irwin M.J., 1994, In: The Local Group. Proceedings of the CTIO-ESO Workshop, La Serena
Kurucz R., 1991, In: Philip A.G., Upgren A.R., Janes P.L. (eds.) Precision Photometry: Astrophysics of the Galaxy. L. Davis Press, Schenectady, p. 27
Lehner N., Keenan F.P., Smoker J.V., et al., 1999, In: New Views of the Magellanic Clouds. Proceedings IAU 190, in press
Lennon D.J., Brown P.J.F., Dufton P.L., 1988, A&A 195, 208
Lennon D.J., Dufton P.L., Mazzali P.A., Pasian F., Marconi G., 1996, A&A 314, 243
Lequeux J., 1984, In: Structure and evolution of the Magellanic Clouds. Proceedings IAU Symp. 108, Reidel, Dordrecht, p. 67
Luks T.H., Rohlfs K., 1992, A&A 263, 41
Massey P., 1997, A User's Guide to CCD Reductions with IRAF, NOAO Laboratory
Massey P., Valdes F., Barnes J., 1992, A User's Guide to Reducing Slit Spectra with IRAF, NOAO Laboratory
Mathewson D.S., Schwarz M.P., Murray J.D., 1977, ApJ 217, L5
Murai T., Fujimoto M., 1980, PASJ 32, 581
Napiwotzki R., Schönberner D., Wenkse V., 1993, A&A 268, 653
Rolleston W.R.J., 1999, A&AS submitted
Rolleston W.R.J., Dufton P.L., Fitzsimmons A., Howarth I.D., Irwin M.J., 1993, A&A 277, 10
Rolleston W.R.J., Brown P.J.F., Dufton P.L., Howarth I.D., 1996, A&A 315, 95
Rolleston W.R.J., Hambly N.C., Dufton P.L., et al., 1997, MNRAS 290, 422
Seaton M.J., 1979, MNRAS 187, 73
Stathakis R.A., Johnston H.M., 1997, The RGO Spectrograph Manual. AAO UM 2.3
Tody D., 1986, IRAF User Manual, NOAO Laboratory
Toomre A., Toomre J., 1972, ApJ 178, 623
Udalski A., Szymański M., Kubiak M., et al., 1998, Acta Astron., in press
Valdes F., 1992, A Guide to the Slit Spectra Reduction Task DOSLIT, NOAO Laboratory
Venn K.A., 1998, In: Chu Y.H., Suntzeff N. (eds.) New Views on the Magellanic Clouds. ASP Conf. Series, San Francisco
Venn K.A., 1999, ApJ, in press
Vidal C.R., Cooper J., Smith E.W., 1973, ApJS 25, 37
Wayte S.R., 1990, ApJ 355, 473
Wayte S.R., 1991, In: Haynes R., Milne D. (eds.) The Magellanic Clouds. Proceedings IAU Symp. 148, Kluwer, Dordrecht, p. 15
Westerlund B.E., 1990, A&AR 2, 27